First-principles calculations of the electronic structure of iron-pnictide $EuFe_2(As,P)_2$ superconductors: Evidence for antiferromagnetic spin order

Wei Li,[1,2] Jian-Xin Zhu,[3] Yan Chen,[1] and C. S. Ting[2]

[1]*Department of Physics and State Key Laboratory of Surface Physics, Fudan University, Shanghai 200433, China*

[2]*Texas Center for Superconductivity and Department of Physics, University of Houston, Houston, Texas 77204, USA*

[3]*Theoretical Division and Center for Integrated Nanotechnologies, Los Alamos National Laboratory, Los Alamos, New Mexico 87545, USA*

(Received 18 August 2012; revised manuscript received 23 September 2012; published 10 October 2012)

By using the first-principles electronic and magnetic structure calculations for the iron pnictides $EuFe_2As_2$ and $EuFe_2P_2$, we find that the ground state of $EuFe_2As_2$ is a collinear antiferromagnetic (AFM) order in the Fe layer and an A-type AFM order with Eu spin lying in the basal plane (along 110), while for $EuFe_2P_2$ the Fe ions do not carry local moment but the Eu ones order ferromagnetically pointing along the c axis (along 001), which are in good agreement with experiments. We further find that the magnetic order in Fe layer is closely related to the Fe-As-Fe bond angle. When the Fe-As-Fe bond angle decreases to a small value, the system favors ferromagnetic order.

DOI: 10.1103/PhysRevB.86.155119 PACS number(s): 74.20.Pq, 74.25.Ha, 74.70.Xa, 76.30.Kg

I. INTRODUCTION

The search for high-temperature superconductivity and novel superconducting mechanism is one of the most challenging tasks in condensed matter community and material physics. The discovery of superconductivity in iron-based materials, such as 1111-type ROFeAs (R = rare earth),[1] 122-type BFe$_2$As$_2$ (B = Ba, Sr, or Ca),[2] 111-type AFeAs (A = alkali metal),[3] 11-type α-FeSe(Te),[4] and new type $K_xFe_{2-y}Se_2$,[5] has generated significant interests in recent years. These materials share the same tetrahedral structure with the divalent iron square planes and antiferromagnetically ordered poor metal phase. The band structure calculations show that the states near the Fermi level are mainly coming from Fe 3d orbitals with only modest hybridization of ligand-p orbitals.[6,7] Most of these compounds were reported to show superconductivity, which is induced by suppressing the magnetic order in their parent compounds after doping or under high pressure.

The discovery of iron-based superconductivity has also brought about new findings on the interplay of superconductivity and ferromagnetism.[8–12] When these alkaline and/or alkaline-earth (named the S state) elements are substituted by the rare-earth ones, i.e., $EuFe_2As_2$[13–15] and $EuFe_2P_2$,[16–18] the long-range magnetic order emerges in the Eu layer due to the localized f moment. It was found that there is a spin-density wave order in the Fe layer together with a structural transition at 190 K and an A-type antiferromagnetic (AFM) order [ferromagnetic (FM) ordered in layers and AFM ordered between layers] on the Eu^{2+} ions at 19 K in $EuFe_2As_2$. By contrast, the Fe layer does not carry local moments while the Eu^{2+} spins order ferromagnetically (the Eu^{2+} moments tilt a little angle of 20° from the c axis) at 27 K in $EuFe_2P_2$. This behavior so far has not been understood. Surprisingly, doping P into $EuFe_2As_2$[19–22] without introducing holes or electrons leads to a scenario generally referred to as "chemical pressure."Both the superconductivity coming from Fe 3d electrons and FM order on the Eu ions can be achieved when the Fe spin-density wave phase is suppressed by P doping. This result indicates the coexistence of superconductivity and ferromagnetism. However, the optical[14] and the photoemission[23] experiments seem to reveal that the FeAs(P) superconducting layer is decoupled from the Eu layer.

In this paper, we report on the detail investigation of the electronic and magnetic structures by performing the first-principles calculations for the $EuFe_2As_2$ and $EuFe_2P_2$. First, our calculations show that the ground state is a collinear AFM (CAF) order with Fe local moments 1.92 μ_B in the Fe layer and an A-type AFM order in the Eu layer with Eu spins lying in the basal plane (along 110) in $EuFe_2As_2$. In contrast, the ions in Fe layer favor a paramagnetism while the Eu ones favor FM order with spin pointing along the c axis (along 001) in $EuFe_2P_2$. These results are in good agreement with experiments. We also calculate the ground-state energies as a function of the Fe-As-Fe bond angle and show that the magnetic order in Fe layers is correlated tightly to the Fe-As-Fe bond angle. It is interesting to point out that when decreasing the Fe-As-Fe bond angle to a small value, the FM order becomes most favorable.

The structure of this paper is as follows. In Sec. II, we present the theoretical methods and results. Finally, in Sec. III, we summarize our main conclusions.

II. THEORETICAL METHODS AND RESULTS

The first-principles calculations presented in this work were performed using the all-electron full potential linear augmented plane wave plus local orbitals (FP-LAPW + lo) method[24] as implemented in the WIEN2K code.[25] The exchange-correlation potential was calculated using the generalized gradient approximation (GGA) as proposed by Pedrew, Burke, and Ernzerhof.[26] We have included the strong Coulomb repulsion in the Eu-4f orbitals on a mean-field level using the GGA + U approximation, applying the atomic limit double-counting scheme. There exist no spectroscopy data for $EuFe_2As_2$ and $EuFe_2P_2$, therefore, throughout this work, we have used a U of 8 eV, which is the standard value for an Eu^{2+} ion. The results were checked for consistency with varying U values. We did not apply U to the itinerant Fe 3d orbitals. Additionally, the spin-orbit coupling is also included with the second variational method in the Eu 4f orbitals. These

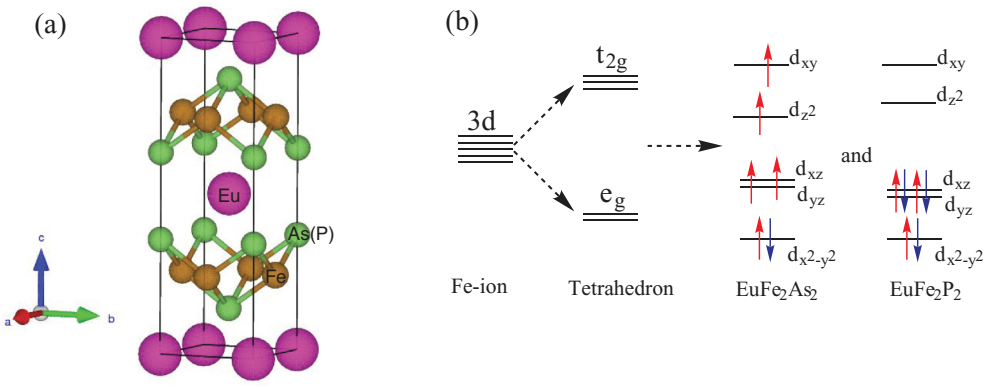

FIG. 1. (Color online) (a) The schematic crystal structure of $EuFe_2As(P)_2$; (b) Sketch of the Fe $3d$ orbital levels for $EuFe_2As_2$ and $EuFe_2P_2$. The coordinate system is chosen such that the x and y axis point from the Fe atom towards the n.n.n. Fe atoms.

calculations were performed using the experimental crystal structure,[16] which is shown in Fig. 1(a). In Fig. 1(b), we sketch the Fe $3d$ orbital levels for $EuFe_2As_2$ and $EuFe_2P_2$ based on our calculations and they will be discussed in detail below.

We start with the study of electronic properties of both $EuFe_2As_2$ and $EuFe_2P_2$ in the quenched paramagnetic state, which means no spin polarization is allowed on the Fe ions in the calculations. Such a study can provide a reference for studying magnetization states, and, by analyzing the density of states (DOS) at the Fermi level, we can infer whether the magnetic state is favored. From Fig. 2, we can see that, in comparison to two systems, the DOS of both systems are quite similar. Since the Eu $4f$ states are quite localized, the Eu ions are in a stable $2+$ valence state with a half $4f$ shell (the magnetic moment on Eu is about 6.9 μ_B). Apart from the Eu $4f$ states, the remaining DOS are almost identical with that of other iron-based superconductors[27–30] and exhibit the typical characteristics of layered structures. We notice that the DOS can be divided into two parts: The lower part (2 eV below the Fermi level) consists of these bands formed through the bonding between the Fe $3d$ and As $4p$ (P-$3p$) orbitals. The p-d hybridization between As (P) and Fe is sizable. The upper part is basically composed of the Fe $3d$ orbitals ranging from -2 eV to 2 eV centered at the Fermi level. However, it is interesting to note that the DOS coming from Fe $3d$ orbitals exhibits a peak at the Fermi level in $EuFe_2As_2$, while the DOS in $EuFe_2P_2$ exhibits a dip at the Fermi level. The corresponding value of DOS at the Fermi level is $N_{As}(E_f) = 2.15$ and $N_P(E_f) = 1.0$ states per eV per Fe atom, respectively. According to the Stoner criterion,[31] while magnetism may occur with lower values of the DOS, it must occur within a band picture if the Stoner criterion, $N(E_f)I > 1$, is met [the nonmagnetic (NM) electronic structure becomes unstable against FM state in this case], where I is the Stoner parameter, which takes values of 0.7–0.9 eV for ions near the middle of the $3d$ series (note that the effective I can be reduced by hybridization). Therefore, the NM state is stable in $EuFe_2P_2$, while in $EuFe_2As_2$ the NM state is unstable against the magnetic states.

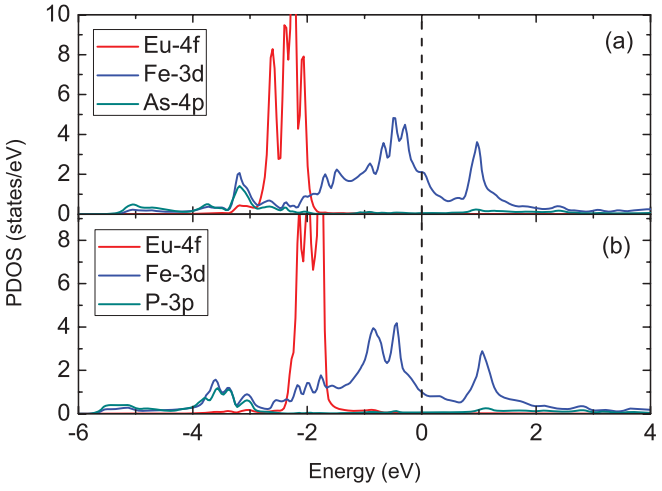

FIG. 2. (Color online) The PDOS on the Eu, Fe, and As(P) elements per unit cell of $EuFe_2As_2$ (a) and $EuFe_2P_2$ (b) in the NM state in Fe layer and FM interaction between the intralayer Eu spins in Eu layer. The unfilled Eu $4f$ states are at about 10 eV above the Fermi level. The Fermi energy is set to zero (black dash line).

To explore the magnetic structure of the $EuFe_2As_2$, we have calculated three different possible magnetic states in the Fe layer with FM, Néel-AFM, and CAF order (align FM order along a direction and AFM order along the other direction in the Fe-Fe square lattice, similarly to that in LaOFeAs[28]) together with the NM state are calculated. The corresponding total energies of different magnetic states are listed in Table I. It is shown that a CAF order in the Fe layer and an A-type AFM order in the Eu layer is the lowest energy state for $EuFe_2As_2$,

TABLE I. Energetic and magnetic properties of the $EuFe_2As_2$ and $EuFe_2P_2$. Results in the magnetic states together with NM configurations in Fe layer using experimental crystal structures.[16] ΔE (eV) is the total energy difference per iron atom in reference to the NM state, and m_{Fe}/m_{Eu} (μ_B) is the local magnetic moment on Fe.

	$EuFe_2As_2$	$EuFe_2P_2$
	$\Delta E/m_{Fe}/m_{Eu}$	$\Delta E/m_{Fe}/m_{Eu}$
NM	0/0/6.92	0/0/6.90
FM	0.0444/1.95/6.92	−0.0003/0.01/6.90
AFM	−0.0467/1.66/6.92	−0.0003/0.07/6.90
CAF	−0.1382/1.92/6.92	−0.0010/0.07/6.90

which is in good agreement with experiments.[13] The magnetic states for $EuFe_2P_2$ are also calculated to check that the NM state and magnetic states in the Fe layer are almost degenerate, and a FM order in the Eu layer[18] is the most stable state (see Table I). It is interesting to note that a small value moment on Fe comes from the proximate effect of ferromagnetically ordered in Eu layer. Furthermore, by calculating the magnetic exchange coupling between two nearest-neighbor (n.n.) Fe and Eu atoms, J^{NN}_{Eu-Fe} ($J^{NN}_{Eu-Fe} = -1.11$ meV for $EuFe_2As_2$ and -10^{-3} meV for $EuFe_2P_2$) reveals that the Eu and Fe ion layers are almost decoupled, which also agrees with experimental results.[14,23,32] Therefore, we can discuss independently the magnetism on two subsystems.

We now proceed to elaborate why there is no magnetic moment on Fe ions when As atoms are substituted by P ones. From the viewpoint of ligand field theory, the Fe layer is coordinated by the As(P) tetrahedron, and the crystal field will normally split the five $3d$ orbitals into the low-lying twofold e_g orbitals and up-lying threefold t_{2g} orbitals opposite the octahedral case, as shown in Fig. 1(b). Actually, in both $EuFe_2As_2$ and $EuFe_2P_2$, the As(P) tetrahedron is squeezed down (the Fe-As-Fe angle is 110.11° for $EuFe_2As_2$ and 116.71° for $EuFe_2P_2$) from the normal shape (the normal angle is 109.47°). This squeezing will further split the e_g and t_{2g} manifolds, complicating the final orbital distributions significantly. However, when taking the Coulomb interaction into account, the actually instance by analyzing the project DOS (PDOS) into Fe five orbitals is opposite that which we expect from a simple tetrahedra crystal field: the low-lying manifold is threefold and the up-lying manifold is twofold. Since the As(P)-p electrons in tetrahedral symmetry are not oriented directly towards the $3d$ orbitals, the energy splitting will be lower than that in the octahedral case. On the other hand, due to the narrow band of $3d$ orbitals, the Hund's coupling energy scale is much larger than that of crystal field splitting. As a result, it is easier to put electrons into the higher energy level of orbitals than it is to put two into the same low-energy orbital. Therefore, the system favors the "high-spin" state. $EuFe_2As_2$ can be realized and is shown in Fig. 1(b). There arises a question that the calculated spin moment is about 2.0 μ_B/Fe, which is much reduced from the expected 4μ_B/Fe. Because the p-d hybridization is sizable,[33] it will dramatically reduce the spin moments.

When As atoms are substituted by P ones, the height between the P and Fe layers will be reduced because the atomic radii of P is much smaller than that of the As atom. As a result, the P tetrahedron will be further squeezed, and the Fe-As-Fe bond angle will be enlarged to a large value (116.71°). The crystal field splitting gap scale will be enhanced dramatically, even be larger than that of Hund's coupling. The electrons on the Fe $3d$ orbitals will pair up and fill the lower-lying orbital. This complex is called "low spin."For the Fe^{2+} ion, the nominal number of $3d$ electrons is 6, the low-lying threefold bands are nearly fully occupied, and the spin moment becomes zero.

To examine the aforementioned discussion, we further calculate the total energies for several possible magnetic states as a function of the internal coordinate of z(As), which is equivalent to a function of the Fe-As-Fe bond angle α by keeping the lattice constants in $EuFe_2As_2$ unchanged. The results are shown in Fig. 3(a). Within a spin-exchange J_1-J_2 model for Fe layers, the corresponding nearest-neighbor (n.n.) exchange interaction J_1 and next-nearest-neighbor (n.n.n.) J_2 values as a function of z are shown in Fig. 3(b). It is shown that both the ground state and the magnetic moment are changed dramatically with a decrease in the bond angle. Since the bond angle is uniquely determined by the lattice constants and the anion height, we put the bond angle of $EuFe_2P_2$ ($\alpha = 116.71°$) into this figure, the ground state is the same as that of $EuFe_2P_2$. Namely. if we only change the Fe-As-Fe bond angle α in $EuFe_2As_2$ to be the same as that of $EuFe_2P_2$, the electronic and magnetic structures can be realized. Therefore, the Fe-As-Fe bond angle α will be increased and the long range AFM ordering will be suppressed as substituting isoelectronic P at As site without introducing any holes or electrons. We further expect that all the parent compounds of iron-based superconductors can be mapped into this picture. The Fe-As-Fe bond angle α uniquely determines the magnetic states due to the crystal symmetries of the tetrahedral structure. Furthermore, some previous experiments[34–38] have indicated a strong relationship between the transition temperature T_c and the Fe-As-Fe bond angle α, that is, the transition temperature T_c becomes maximum when the $FeAs_4$ structure forms a norm tetrahedron except for α-FeSe.[38] This anomalous behavior is interpreted as arising from the spin fluctuations.[39–42]

To form the high-temperature superconductivity, two necessary conditions must be satisfied: (i) a strong pairing interaction, which could be related to the magnetic fluctuations, and (ii) a large DOS at the Fermi level. In Fig. 3(b), it shows that the J_2 value (note: the pairing interaction in Fe-based

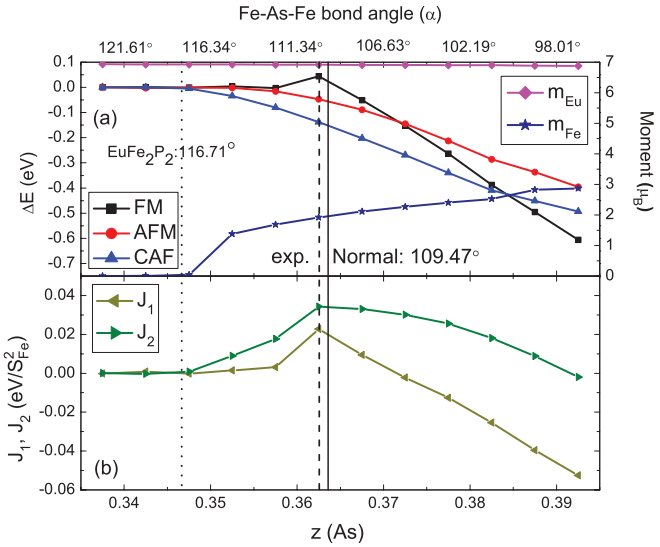

FIG. 3. (Color online) (a) Calculated magnetic moments for europium (m_{Eu}) and iron (m_{Fe}) and the total energy of several magnetic configurations (FM, AFM, CAF, and BCAF) and the difference per iron atom in reference to the NM state (ΔE) as a function of the internal coordinate of z(As). The correspondence to the Fe-As-Fe bond angle α is also labeled. (b) The values of J_1 and J_2 of the J_1-J_2 model in the Fe layer is also evaluated. The sold, dished, and dotted vertical lines represent the normal tetrahedral structure of the FeAs plane (normal: 109.47°), the experimental value (exp.) of internal coordinate z(As), and the same Fe-As-Fe bond angle to that of $EuFe_2P_2$ ($EuFe_2P_2$: 116.71°), respectively.

TABLE II. Energetic properties of the different europium spin-ordered orientations for $EuFe_2As_2$ and $EuFe_2P_2$. Results are the total energy difference per europium atom for different europium spin-ordered directions in the Eu layer.

	$EuFe_2As_2$(meV)	$EuFe_2P_2$(meV)
(100)	0.03893	0.06712
(110)	0	0.02101
(001)	0.01873	0
(111)	0.01493	0.01972

superconductors is mainly determined by the n.n.n. exchange coupling strength J_2) reaches maximum at the normal $FeAs_4$ tetrahedral structure. Therefore, the transition temperature T_c can have the largest value when the $FeAs_4$ structure forms a norm tetrahedron. However, for the undoped α-FeSe compound, it has a relatively low DOS intensity at the Fermi level [with $N(E_f) = 0.95$ states eV per Fe ion],[43] the transition temperature is indeed not so high. It is interesting to point out that the ground state favors FM order when the Fe-As-Fe bond angle decreases to a small value ($\alpha < 100^\circ$). Considering its close vicinity to the FM instability, the present system is very similar to Sr_2RuO_4,[44] where strong FM fluctuations favor triplet pairing. When the FM order is suppressed, a p-wave superconductivity may emerge. Following such a picture, it is possible to realize p-wave superconductors with a tetrahedral structure.

Finally, we turn to discuss the magnetic order in the Eu layer. To quantify the magnetic interactions in Eu layer, an effective Heisenberg model can be modeled as follows:

$$\hat{H} = J_1' \sum_{\langle i,j \rangle} \vec{S}_i \cdot \vec{S}_j + J_\perp \sum_{\langle i,j \rangle} \vec{S}_i \cdot \vec{S}_j,$$

where $\vec{S}$ is the magnitude of Eu spin and $\langle i,j \rangle$ denotes the summation over the n.n. sites. The parameters J_1' and $J_\perp$ are the n.n. intralayer and interlayer exchange interactions, respectively. From the calculated energy datas, we find that for $EuFe_2As_2$ $J_1' = -1.04$ meV and $J_\perp = 0.09$ meV, while for $EuFe_2P_2$ $J_1' = -1.21$ meV and $J_\perp = -0.26$ meV. The calculations (see Table II) also show that an A-type AFM order in the Eu layer with Eu $4f$ spins lies in the basal plane (along 110) for $EuFe_2As_2$, while the Eu layer favors FM order with Eu $4f$ spins pointing along the c axis (along 001) for $EuFe_2P_2$. These results are in good agreement with experiments but differing a bit from the Mössbauer spectroscopy measurement, which showed that the Eu spin tilts 20° from the c axis for $EuFe_2P_2$. This difference can be interpreted as thermodynamic fluctuations at finite temperature. The AFM-FM in the Eu layer transition can be explained by the indirect RKKY interaction [$J_R \sim (J^{NN}_{\text{Fe-Eu}})^2 N(E_F)$] between interlayer Eu $4f$ electrons mediated by the d-f coupling $J^{NN}_{\text{Fe-Eu}}$ in the ordered phases.[11,16] Intuitively, the interlayer exchange coupling $J_\perp$ is given by $J_\perp = J_\perp^0 + J_R$, with $J_\perp^0$ being the weak direct FM interaction between interlayer Eu moments. When the As atom is substituted by P, the calculated d-f exchange coupling value mediated by the As(P) states decreases from a small value ($J^{NN}_{\text{Fe-Eu}} = -1.11$ meV) to almost zero ($J^{NN}_{\text{Fe-Eu}} = -10^{-3}$ meV), leading to a sign change in $J_\perp$.

III. CONCLUSION

In conclusion, we have performed the first-principles calculations for $EuFe_2As_2$ and $EuFe_2P_2$ and shown that the ground state is a CAF order in the Fe layer and an A-type AFM order with Eu spin lying in the basal plane (along 110) in $EuFe_2As_2$, while the Fe ions do not carry local moment but the Eu spins order ferromagnetically, pointing along the c axis (along 001), results which are in good agreement with experiments. The magnetic exchange couplings have also been calculated, which shows an almost magnetically decoupling between the Fe and Eu layers. We have also shown that the Fe-As-Fe bond angle controls effectively the magnetic order in the Fe layers. In particular, we show that when the Fe-As-Fe bond angle decreases to a small value, the system favors the FM order.

ACKNOWLEDGMENTS

We thank R. B. Tao, J. P. Hu, Z. Fang, S. H. Pan, H. J. Xiang, G. Xu, and J.-P. Julien for helpful discussions. This work was supported by the Texas Center for Superconductivity at the University of Houston and by the Robert A. Welch Foundation under Grant No. E-1146 (W.L. and C.S.T.), by the National Nuclear Security Administration of the US Department of Energy at LANL under Contract No. DE-AC52-06NA25396 and the US DOE Office of Basic Energy Sciences (J.-X.Z.), and by the National Natural Science Foundation of China (Grant No. 11074043) and the State Key Programs of China (Grants No. 2009CB929204 and No. 2012CB921604) (Y.C.). W.L. also gratefully acknowledges financial support by the Research Fund of Fudan University for the Excellent Ph.D. Candidates.

[1] Y. Kamihara, T. Watanabe, M. Hirano, and H. Hosono, J. Am. Chem. Soc. **130**, 3296 (2008).
[2] M. Rotter, M. Tegel, and D. Johrendt, Phys. Rev. Lett. **101**, 107006 (2008).
[3] X. C. Wang, Q. Q. Liu, Y. X. Lv, W. B. Gao, L. X. Yang, R. C. Yu, F. Y. Li, and C. Q. Jin, Solid State Commun. **148**, 538 (2008).
[4] F.-C. Hsu, J.-Y. Luo, K.-W. Yeh, T.-K. Chen, T.-W. Huang, P. M. Wu, Y.-C. Lee, Y.-L. Huang, Y.-Y. Chu, D.-C. Yan, and M.-K. Wu, Proc. Natl. Acad. Sci. USA **105**, 14262 (2008).
[5] J. Guo, S. Jin, G. Wang, S. Wang, K. Zhu, T. Zhou, M. He, and X. Chen, Phys. Rev. B **82**, 180520(R) (2010).
[6] D. J. Singh and M. H. Du, Phys. Rev. Lett. **100**, 237003 (2008).
[7] W. Li, J. Li, J.-X. Zhu, Y. Chen, and C. S. Ting, Europhys. Lett. **99**, 57006 (2012).
[8] G. F. Chen, Z. Li, D. Wu, G. Li, W. Z. Hu, J. Dong, P. Zheng, J. L. Luo, and N. L. Wang, Phys. Rev. Lett. **100**, 247002 (2008).
[9] S. Chi, D. T. Adroja, T. Guidi, R. Bewley, S. Li, J. Zhao, J. W. Lynn, C. M. Brown, Y. Qiu, G. F. Chen, J. L. Lou, N. L. Wang, and P. Dai, Phys. Rev. Lett. **101**, 217002 (2008).
[10] C. de la Cruz, W. Z. Hu, S. Li, Q. Huang, J. W. Lynn, M. A. Green, G. F. Chen, N. L. Wang, H. A. Mook, Q. Si, and P. Dai, Phys. Rev. Lett. **104**, 017204 (2010).

[11] Y. Luo, Y. Li, S. Jiang, J. Dai, G. Cao, and Z.-A. Xu, Phys. Rev. B **81**, 134422 (2010).
[12] W. Li, S. Dong, C. Fang, and J. Hu, Phys. Rev. B **85**, 100407(R) (2012).
[13] Y. Xiao, Y. Su, M. Meven, R. Mittal, C. M. N. Kumar, T. Chatterji, S. Price, J. Persson, N. Kumar, S. K. Dhar, A. Thamizhavel, and Th. Brueckel, Phys. Rev. B **80**, 174424 (2009).
[14] D. Wu, N. Barisic, N. Drichko, S. Kaiser, A. Faridian, M. Dressel, S. Jiang, Z. Ren, L. J. Li, G. H. Cao, Z. A. Xu, H. S. Jeevan, and P. Gegenwart, Phys. Rev. B **79**, 155103 (2009).
[15] M. A. Sillanpaa, R. Khan, T. T. Heikkila, and P. J. Hakonen, Phys. Rev. B **84**, 195433 (2011).
[16] C. Feng, Z. Ren, S. Xu, S. Jiang, Z. A. Xu, G. Cao, I. Nowik, I. Felner, K. Matsubayashi, and Y. Uwatoko, Phys. Rev. B **82**, 094426 (2010).
[17] D. H. Ryan, J. M. Cadogan, S. Xu, Z. A. Xu, and G. Cao, Phys. Rev. B **83**, 132403 (2011).
[18] L. Hua, J. M. Shen, Q. L. Zhu, and L. Chen, Physica B **406**, 4687 (2011).
[19] Z. Ren, Q. Tao, S. Jiang, C. Feng, C. Wang, J. Dai, G. Cao, and Z. A. Xu, Phys. Rev. Lett. **102**, 137002 (2009).
[20] G. Cao, S. Xu, Z. Ren, S. Jiang, C. Feng, and Z. A. Xu, J. Phys.: Condens. Matter **23**, 464204 (2011).
[21] H. S. Jeevan, Z. Hossain, D. Kasinathan, H. Rosner, C. Geibel, and P. Gegenwart, Phys. Rev. B **78**, 052502 (2008).
[22] H. S. Jeevan, D. Kasinathan, H. Rosner, and P. Gegenwart, Phys. Rev. B **83**, 054511 (2011).
[23] B. Zhou, Y. Zhang, L.-X. Yang, M. Xu, C. He, F. Chen, J.-F. Zhao, H.-W. Ou, J. Wei, B.-P. Xie, T. Wu, G. Wu, M. Arita, K. Shimada, H. Namatame, M. Taniguchi, X. H. Chen, and D. L. Feng, Phys. Rev. B **81**, 155124 (2010).
[24] D. J. Singh and L. Nordstrom, *Planewaves, Pseudopotentials, and the LAPW Method*, 2nd ed. (Springer-Verlag, Berlin, 2006), pp. 1C134.
[25] P. Blaha, K. Schwarz, G. Madsen, D. Kvasnicka, and J. Luitz, in WIEN2K, *An Augmented PlaneWave + Local Orbitals Program for Calculating Crystal Properties*, edited by K. Schwarz (Technical Univievsity Wien, Austria, 2001).
[26] J. P. Perdew, K. Burke, and M. Ernzerhof, Phys. Rev. Lett. **77**, 3865 (1996).
[27] L. Boeri, O. V. Dolgov, and A. A. Golubov, Phys. Rev. Lett. **101**, 026403 (2008).
[28] G. Xu, W. Ming, Y. Yao, X. Dai, S.-C. Zhang, and Z. Fang, Europhys. Lett. **82**, 67002 (2008).
[29] S. Graser, A. F. Kemper, T. A. Maier, H.-P. Cheng, P. J. Hirschfeld, and D. J. Scalapino, Phys. Rev. B **81**, 214503 (2010).
[30] X.-W. Yan, M. Gao, Z.-Y. Lu, and T. Xiang, Phys. Rev. B **84**, 054502 (2011).
[31] D. J. Singh, Phys. Rev. B **78**, 094511 (2008).
[32] Z. Guguchia, A. Shengelaya, A. Maisuradze, L. Howald, Z. Bukowski, M. Chikovani, H. Luetkens, S. Katrych, J. Karpinski, and H. Keller, arXiv:1205.0212 (2012).
[33] F. Ma, Z.-Y. Lu, and T. Xiang, Phys. Rev. B **78**, 224517 (2008).
[34] C.-H. Lee, A. Iyo, H. Eisaki, H. Kito, M. Teresa Fernandez-Diaz, T. Ito, K. Kihou, H. Matsuhata, M. Braden, and K. Yamada, J. Phys. Soc. Jpn. **77**, 083704 (2008).
[35] J. Zhao, Q. Huang, C. de la Cruz, S. Li, J. W. Lynn, Y. Chen, M. A. Green, G. F. Chen, G. Li, Z. Li, J. L. Luo, N. L. Wang, and P. Dai, Nat. Mater. **7**, 953 (2008).
[36] Y. Mizuguchi, Y. Hara, K. Deguchi, S. Tsuda, T. Yamaguchi, K. Takeda, H. Kotegawa, H. Tou, and Y. Takano, Supercond. Sci. Technol. **23**, 054013 (2010).
[37] G. Garbarino, R. Weht, A. Sow, A. Sulpice, P. Toulemonde, M. Alvarez-Murga, P. Strobel, P. Bouvier, M. Mezouar, and M. Nunez-Regueiro, Phys. Rev. B **84**, 024510 (2011).
[38] K. Horigane, H. Hiraka, and K. Ohoyama, J. Phys. Soc. Jpn. **78**, 074718 (2009).
[39] K. Kuroki, H. Usui, S. Onari, R. Arita, and H. Aoki, Phys. Rev. B **79**, 224511 (2009).
[40] C.-Y. Moon and H. J. Choi, Phys. Rev. Lett. **104**, 057003 (2010).
[41] K. Kuroki, J. Phys. Chem. Sol. **72**, 307 (2011).
[42] K. Kuroki, Solid State Commun. **152**, 711 (2012).
[43] A. Subedi, L. Zhang, D. J. Singh, and M. H. Du, Phys. Rev. B **78**, 134514 (2008).
[44] Y. Maeno, H. Hashimoto, K. Yoshida, S. Nishizaki, T. Fujita, J. G. Bednorz, and F. Lichtenberg, Nature **372**, 532 (1994).